The FASEB Journal article fj.201600784R. Published online November 4, 2016.

THE FASEB JOURNAL • RESEARCH • www.fasebj.org

Development of original metabolically-stable apelin-17 analogs with diuretic and cardiovascular effects

Romain Gerbier,* Rodrigo Alvear-Perez,* Jean-Francois Margathe,† Adrien Flahault,* Pierre Couvineau,* Ji Gao,* Nadia De Mota,* Hubert Dabire,‡ Bo Li,* Emilie Ceraudo,* Annette Hus-Citharel,* Lucie Esteoulle,† Cynthia Bisoo,* Marcel Hibert,† Alain Berdeaux,‡ Xavier Iturrioz,*,[1] Dominique Bonnet,†,[1] and Catherine Llorens-Cortes*,[2]

*Laboratory of Central Neuropeptides in the Regulation of Body Fluid Homeostasis and Cardiovascular Functions, Center for Interdisciplinary Research in Biology, INSERM, Unité 1050, Centre National de la Recherche Scientifique, Unité Mixte de Recherche 7241, College de France, Paris, France; †Laboratory of Therapeutic Innovation, Unité Mixte de Recherche 7200, Centre National de la Recherche Scientifique, University of Strasbourg, Faculty of Pharmacy, Illkirch, France; and ‡INSERM Unité 955, Faculty of Medicine, University of Paris Est, Créteil, France

ABSTRACT: Apelin, a (neuro)vasoactive peptide, plays a prominent role in controlling cardiovascular functions and water balance. Because the *in vivo* apelin half-life is in the minute range, we aimed to identify metabolically stable apelin-17 (K17F) analogs. We generated P92 by classic chemical substitutions and LIT01-196 by original addition of a fluorocarbon chain to the N terminus of K17F. Both analogs were much more stable in plasma (half-life >24 h for LIT01-196) than K17F (4.6 min). Analogs displayed a subnanomolar affinity for the apelin receptor and behaved as full agonists with regard to cAMP production, ERK phosphorylation, and apelin receptor internalization. *Ex vivo*, these compounds induced vasorelaxation of rat aorta and glomerular arterioles, respectively, precontracted with norepinephrine and angiotensin II, and increased cardiac contractility. *In vivo*, after intracerebroventricular administration in water-deprived mice, P92 and LIT01-196 were 6 and 160 times, respectively, more efficient at inhibiting systemic vasopressin release than K17F. Administered intravenously (nmol/kg range) in normotensive rats, these analogs potently increased urine output and induced a profound and sustained decrease in arterial blood pressure. In conclusion, these new compounds, which favor diuresis and improve cardiac contractility while reducing vascular resistances, represent promising candidates for the treatment of heart failure and water retention/hyponatremic disorders.—Gerbier, R., Alvear-Perez, R., Margathe, J.-F., Flahault, A., Couvineau, P., Gao, J., De Mota, N., Dabire, H., Li, B., Ceraudo, E., Hus-Citharel, A., Esteoulle, L., Bisoo, C., Hibert, M., Berdeaux, A., Iturrioz, X., Bonnet, D., Llorens-Cortes, C. Development of original metabolically stable apelin-17 analogs with diuretic and cardiovascular effects. FASEB J. 31, 000–000 (2017). www.fasebj.org

KEY WORDS: vascular reactivity · blood pressure · cardiac contractility · vasopressin and diuresis

Apelin is a bioactive peptide isolated from bovine stomach extracts and identified as the endogenous ligand of the human orphan GPCR, APJ (putative receptor protein related to the angiotensin receptor type 1) (1, 2). Apelin is derived from a single 77-aa precursor, preproapelin, which has a fully conserved C-terminal 17-aa sequence, known as apelin-17 or K17F, in all mammalian species studied, and it includes a C-terminal 13-aa sequence, apelin 13. The glutamine residue at the N terminus of apelin 13 is pyroglutamylated to yield the pyroglutamyl form of apelin-13, or pE13F. Both peptides (K17F and pE13F; see **Table 1** for sequences) are naturally present in rat brain and plasma (3), and they inhibit forskolin-induced cAMP production in cells that express the human (4) or rat apelin receptor (ApelinR) (5, 6). These peptides promote phosphorylation of ERKs, Akt, and p70S6 kinase (7), and are also highly potent inducers of rat ApelinR internalization *via* β-arrestin mobilization (8–10).

Both apelin and its receptor are present in the brain (11, 12) and are strongly expressed in the supraoptic and paraventricular hypothalamic nuclei. Dual labeling studies have shown that apelin and its receptor colocalize with arginine-vasopressin (AVP) in magnocellular neurons

ABBREVIATIONS: 4Br-Phe, 4-bromo-phenylalanine; Aib, α-aminoisobutyric acid; AngII, angiotensin II; ApelinR, apelin receptor; AVP, arginine-vasopressin; BP, blood pressure; BRET, bioluminescence resonance energy transfer; CD, collecting duct; DMF, *N*,*N*-dimethylformamide; EGFP, enhanced green fluorescent protein; FC, fluorocarbon chain; HF, heart failure; HRMS, high-resolution mass spectrometer; MABP, mean arterial blood pressure; NE, norepinephrine; YFP, yellow fluorescent protein

[1] These authors contributed equally to this work.

[2] Correspondence: Laboratory of Central Neuropeptides in the Regulation of Body Fluid Homeostasis and Cardiovascular Functions, Collège de France, INSERM U1050/CNRS UMR7241, 11 Place Marcelin Berthelot, 75005 Paris, France. E-mail: c.llorens-cortes@college-de-france.fr

doi: 10.1096/fj.201600784R

This article includes supplemental data. Please visit *http://www.fasebj.org* to obtain this information.

TABLE 1. *Amino acid sequences of metabolically stable apelin analogs*

Apelin analog	Amino acid sequence
pE13F	pGlu-Arg-Pro-Arg-Leu-Ser-His-Lys-Gly-Pro-Met-Pro-Phe-OH
P26	N-Acetyl-Arg-Pro-Arg-DLeu-Ser-Aib-Lys-DAla-ProNle-Pro(4-Br)Phe-OH
K17F	H-Lys-Phe-Arg-Arg-Gln-Arg-Pro-Arg-Leu-Ser-His-Lys-Gly-Pro-Met-Pro-Phe-OH
P92	N-Acetyl-Lys-Phe-DArg-Arg-DGln-Arg-Pro-Arg-DLeu-Ser-Aib-Lys-DAla-ProNle-Pro(4Br)Phe-OH
LIT01-196	$CF_3(CF_2)_7(CH_2)_2C(O)$-Lys-Phe-Arg-Arg-Gln-Arg-Pro-Arg-Leu-Ser-His-Lys-Gly-Pro-Met-Pro-Phe-OH

within these 2 nuclei (3, 11–13). Central injection of K17F into lactating rats inhibits the phasic firing pattern of AVP neurons, thereby decreasing the release of AVP into the bloodstream and increasing aqueous diuresis (3). In addition, systemic injection of K17F into lactating rats increases aqueous diuresis by decreasing aquaporin-2 insertion into the apical membrane in collecting ducts (CDs). This increase in diuresis is a result of the inhibitory effect of K17F on AVP-induced cAMP production in the CD (14). Thus, the aquaretic effect of apelin is a result not only of a central effect that involves an inhibition of AVP release into the bloodstream, but also of a direct renal effect of apelin on the CD, which counteracts the antidiuretic effect of AVP that is mediated by AVP receptor type 2.

After water deprivation, endogenous levels of AVP and apelin are regulated in opposite directions to optimize systemic AVP release, which is required to prevent additional water loss in the kidneys (3, 15). This pattern—with the opposite regulation of plasma apelin and AVP levels by osmotic stimuli—is conserved in humans (16), and an abnormal apelin/AVP balance may contribute to water retention in hyponatremic patients with inappropriate antidiuretic hormone syndrome and chronic heart failure (HF) (17).

Apelin and its receptor are also present in the cardiovascular system, the heart, kidney, and blood vessels (18). When administered systemically to rats, apelin decreases arterial blood pressure (BP) (9, 19) *via* a NO-dependent mechanism (19). Consistent with these data, ApelinR-deficient mice have an exaggerated pressor response to systemic angiotensin II (AngII), which suggests a counter-regulatory effect of apelin on AngII (20). Similarly, in humans, apelin causes NO-dependent arterial vasodilation *in vivo* (21, 22). Moreover, apelin improves myocardial contractility and reduces cardiac loading in rodents (23, 24). Apelin-deficient mice that are subjected to chronic pressure overload as a result of surgical constriction of the aorta develop severe, progressive HF (25). Loss of apelin in apelin-KO mice exacerbates myocardial infarction adverse remodeling and ischemia-reperfusion injury (26). Down-regulation of the apelin system is thus accompanied by a decline in cardiac performance. In parallel, infusion of pE13F for 6 h in humans with chronic HF increases cardiac index (27).

Thus, apelin plays a key role in maintaining body fluid homeostasis and cardiovascular functions, and its receptor is an interesting potential new target for therapeutic research and drug design. Because the *in vivo* half-life of apelin is in the minute range, development of metabolically stable ApelinR agonists to favor diuresis and to improve cardiac function at the same time as reducing vascular resistance would therefore be particularly useful for the treatment of HF, water retention, and/or hyponatremic disorders.

Several studies have focused on the development of synthetic apelin agonists *via* cyclization (28, 29), PEGylation (30), lipopeptide synthesis (31), and production of apelin analogs that are focused on pE13F (32–35). In parallel, we have set up an original FRET-based assay that, when applied to ApelinR, enabled the discovery of the first nonpeptidic ApelinR agonist, E339-3D6 (6). However, this compound exhibited a high molecular weight and behaved as a partial agonist with regard to cAMP production and as a full agonist with regard to ApelinR internalization (6). As metabolically stable peptides, such as liraglutide for type 2 diabetes, desmopressin acetate for central diabetes insipidus and hemorrhage, plenaxis for prostate cancer, and sandostatin for acromegalia (36, 37), are now used in clinic, we aimed to identify metabolically stable K17F analogs that would be more powerful than previously described pE13F analogs. For this purpose, we performed structure-activity studies on K17F in which each amino acid was replaced by its D-isomer or an unnatural amino acid. In parallel, an original, previously undescribed strategy was used to add a fluorocarbon chain (FC) to the N-terminal amino group of K17F. Both strategies led to isolation of several compounds, the most potent of which were 2 K17F analogs, P92 and LIT01-196, that had a subnanomolar affinity for rat ApelinR, behaved as full agonists in several functional tests, and exhibited a much higher plasma stability than that of K17F. We evaluated the effects of these compounds on vessel reactivity and cardiac contractility *ex vivo* and their effects on systemic AVP release, diuresis, and arterial BP *in vivo*.

MATERIALS AND METHODS

Drugs and antibodies

K17F, pE13F, and derivatives of these 2 forms of apelin were synthesized by PolyPeptide Laboratories (Strasbourg, France) and GL Biochem (Shanghai, China), respectively. Inactin [5-ethyl-2-(1′-methylpropyl)-2-thiobarbiturate] was obtained from RBI (Natick, MA, USA), and [^{125}I]-pE13F (monoiodinated on Lys^8 with Bolton-Hunter reagent) was purchased from PerkinElmer (Wellesley, MA, USA).

Chemical synthesis of LIT01-196

LIT01-196 (20.6 mg) was obtained (38) as a white solid [t_R = 4.07 min; > 98% purity at 220 nm; high-resolution mass spectrometer (HRMS; electrospray ionization) calculated

for $C_{107}H_{164}F_{17}N_{34}O_{21}S$ ([M+ 5H]$^{5+}$) 523.24519; observed, 523.24507]. Boc-L-Lys(Fmoc)-FR(Pbf)R(Pbf)QR(Pbf)PR(Pbf)LS(tBu)H(Trt)K(Boc)GPMPF-Wang resin (1 equiv, 15 μmol) was produced by a classic Fmoc/tbutyl strategy. The resin was then allowed to swell in *N*,*N*-dimethylformamide (DMF), and the excess solvent was removed by filtration. A solution of piperidine in DMF (20% v/v^{-1} ml) was added and mixture was incubated at room temperature for 15 min with shaking. Solution was drained off and the operation was repeated for another 15 min. Resin was washed with DMF and CH_2Cl_2. In a separate vial, di-isopropylethylamine (DIPEA; Hünig's base; 5 equiv, 13.1 μl, 75 μmol) was added to a solution of 2H,2H,3H,3H-perfluorononanoic acid (2 equiv, 14.8 mg, 30 μmol), 2-(1H-benzotriazol-1-yl)-1,1,3,3-tetramethyluronium hexafluorophosphate (HBTU; 2 equiv, 11.3 mg, 30 μmol), and 1-hydroxybenzotriazole (HOBt; 2 equiv, 4.6 mg, 30 μmol) in DMF (1 ml). Mixture was stirred at room temperature for 1 min and then added to the resin. Mixture was incubated for 90 min at room temperature with shaking. Solution was drained off and the procedure was repeated for a further 90 min. Resin was washed with DMF, CH_2Cl_2, and diethyl ether and dried under a vacuum. Dried resin was treated with TFA/phenol/thioanisole/1,2-ethanedithiol/Me2S/water/NH_4I, 81/5/5/2.5/2/3/1.5 (2 ml), and mixture was incubated at room temperature for 3 h with shaking. Solution was collected and beads were washed with TFA. Solution was concentrated under a vacuum and the crude product was purified by semipreparative reverse-phase HPLC. Freeze-drying yielded the lead compound (20.6 mg, 49%) as a white solid [t_R = 4.07 min; > 98% purity at 220 nm; HRMS (electrospray ionization) calculated for C107H164F17N34O21S ([M+ 5H]5+) 523.24519; observed, 523.24507].

Animals

Male Swiss mice (18–20 g), male and female Sprague Dawley rats (130–180 g), and male Wistar rats (275–325 g) were maintained under 12-h light/dark cycles with free access to food and water. Animals used were obtained from Charles River Laboratories (L'Arbresle, France) and Janvier (Le Genest-St-Isle, France). All animal experiments were carried out in accordance with current institutional guidelines for the care and use of experimental animals.

Stability of pE13F, K17F, P26, P92, and LIT01-196 in mouse plasma

For each compound, stock solution (100 μM in water) was diluted in plasma to a final concentration of 5 μM. Resulting mixture was incubated at 37°C for various times, from T0 to T4 h. The reaction was stopped with addition of 1 volume of ice-cold 0.1% TFA in acetonitrile at the end of the incubation period. Sample was vortexed and centrifuged and liquid chromatography-mass spectrometry was performed on the supernatant. Analyses were performed on a Kinetex RP-C18 column (2.6 μm, 100 Å, 50 × 4.6 mm) with a linear gradient (solvent B in solvent A; solvent A: water/0.05% TFA; solvent B: acetonitrile; flow rate of 2 ml/min; detection at 358 nm). The percentage of the test compound that remained relative to that present at T0 was determined by monitoring the peak area of the chromatogram. Half-life ($T_{1/2}$) was estimated from the slope of the initial linear range of the logarithmic curve of the compound remaining (%) against time, assuming first-order kinetics.

Membrane preparations and radioligand binding experiments

Membranes from CHO cells that stably expressed rat ApelinR-EGFP (enhanced green fluorescent protein; clone B70) were prepared as previously described (6). We compared affinities of K17F, pE13F, and apelin analogs by performing classic binding studies with radioiodinated pE13F as previously described (6).

cAMP assay

We quantified cAMP production with the cAMP dynamic 2 assay kit (Cisbio Bioassays, Codolet, France) by using homogeneous time-resolved fluorescence technology as previously described (39).

Internalization assay

CHO cells that stably expressed rat ApelinR-EGFP (clone B70) were used to seed glass coverslips that were coated with polylysine (0.01% wt/v; Sigma-Aldrich, St. Quentin, France) to 20% confluence. Internalization was triggered by incubating cells with various concentrations of K17F, pE13F, or an apelin analog at 37°C for 20 min. Cells were then mounted in Aquapolymount (Polysciences, Warrington, PA, USA) for confocal microscopy analysis. We quantified ligand-induced rat ApelinR-EGFP internalization by confocal microscopy coupled to digital image analysis as previously described (6).

β-Arrestin 2 recruitment assay

*R*luc8–β-arrestin 2–encoding plasmid (details of the construct are provided in the Supplemental Data) and the yellow fluorescent protein (YFP)–tagged wild-type rat ApelinR construct were used to cotransfect HEK293T cells. Recruitment of β-arrestin 2 by ApelinR was monitored by bioluminescence resonance energy transfer (BRET) 1. RLuc8-B-arrestin 2-encoding plasmid and the YFP-tagged wild-type rat ApelinR construct were used to cotransfect HEK293T cells. Cells were transferred to a white 96-well Optiplate (PerkinElmer) at a density of 40,000 cells/well, 24 h after transfection. RLuc substrate, coelentherazine H (2.5 mM; Nanolight Technology, Pinetop, AZ, USA), was added 5 min before reading. For kinetic studies, cells were treated with vehicle or apelin peptides (at 1 μM) and the plates were immediately subjected to repeated reading (every 15 s) for 15 min with the EnVision Xcite multilabel reader (PerkinElmer). For dose-response experiments, cells were exposed to various concentrations (1 pM to 100 μM) of apelin peptides for 15 min. BRET1 signal was determined by calculating the ratio of the light emitted at 522–537 nm (YFP) with that emitted at 478–492 nm (Luciferase).

ERK1/2 phosphorylation assay

CHO cells that stably expressed ApelinR-EGFP were plated in 96-well plates at a density of 40,000 cells/well and grown for 24 h. Cells were starved by culture for 16 h in serum-free medium. Cells were then treated with pE13F, K17F, P26, P92, or LIT01-196 for various times for time-course experiments, and with different concentrations of peptides (from 10 pM to 10 μM) for 10 min for dose-response experiments. ERK1/2 phosphorylation was measured with the ERK1/2 Alphascreen Surefire kit in accordance with manufacturer instructions (PerkinElmer).

Preparation of aortic rings and isometric tension recording

Experiments were performed as described previously (6, 40). Rat aortic rings were prepared by equilibration in physiological salt solution for 120 min under a resting tension of 2 g. During the

equilibration period, rings were washed every 30 min. A first relaxation in acetylcholine (100 μM) was used to check the integrity of the endothelium in rings that were precontracted with norepinephrine (NE; 3 μM). Rings were rinsed with physiological salt solution to ensure a return to baseline tension and were then equilibrated for 90 min. At the end of this equilibration period, cumulative concentration–response curves (1 pM to 1 μM) for K17F, P92, and LIT01-196 were constructed after precontraction with NE (3 μM). Each concentration of the drug was added at the maximal effect of the previous concentration. Concentration–response curves were continuously recorded on a PC with an IOX v. 2.4 data acquisition system (Emka Technologies, Paris, France) for further analysis (Datanalyst v2.1; Emka Technologies).

Microdissection and measurement of glomerular arteriole diameter

Experiments were performed as described previously (Supplemental Data) (8).

Isolated perfused rat heart preparation

Animals were anesthetized with pentobarbital (50 mg/kg, i.p.). Heparin (200 IU/kg) was administered *via* the femoral vein. Hearts were rapidly excised and arrested in ice-cold Krebs-Henseleit solution that contained 118.5 mM NaCl, 4.75 mM KCl, 1.19 mM $MgSO_4$, 1.2 mM KH_2PO_4, 24 mM $NaHCO_3$, 1.4 mM $CaCl_2$, and 11 mM glucose. Hearts were then mounted on a perfusion apparatus, and a fluid-filled isovolumic balloon constructed from cling film was introduced into the left ventricle and inflated to give a preload of 8–10 mmHg. Left ventricular pressure was recorded continuously on a computer. After a 20-min equilibration period, hearts were treated by addition of drugs to the perfusate, which was delivered with an infusion pump (Pump 11; Harvard Apparatus, Holliston, MA, USA) at a rate of 100 μl/min for 30 min (see the Supplemental Data).

Intracerebroventricular injections in mice and AVP radioimmunoassay

K17F (1 μg), P92 (0.01–1 μg), and LIT01-196 (0.0001–1 μg) were administered *via* the intracerebroventricular route in conscious mice that had free access to water or that were deprived of water for 24 h, as previously described (3). Animals were killed 1 min after injection and trunk blood (0.5–1 ml) was collected in chilled tubes that contained 50 μl of 0.3 M EDTA pH 7.4. AVP concentrations were determined as previously described (3) on 0.2 ml of plasma by radioimmunoassay with a specific AVP-[Arg^8] Ab (Peninsula Laboratories International, San Carlo, CA, USA) and [^{125}I]-(Tyr^2Arg^8)-AVP (PerkinElmer) as a tracer.

Intravenous injections in anesthetized rats and urine output measurement

Sprague-Dawley female virgin rats (220–250 g) were anesthetized with inactin (100 mg/kg, i.p.). A catheter was inserted into the femoral vein and a bladder catheter was inserted through the urethra. In all animals, after a stabilizing period of 30 min, intravenous administration of 400 μl of saline was performed to determine baseline values of diuresis rate for 2 h. Rats then received 400 μl of either saline or 5 nmol of P92 (20 nmol/kg), and diuresis rate was recorded for another 2-h period. Diuresis rate was expressed in μl per min per 100 g body weight.

BP recording in anesthetized Wistar rats

Wistar rats were anesthetized with inactin (100 mg/kg, i.p.). K17F, P92, or LIT01-196 was dissolved in 0.2 ml Krebs buffer (118.5 mM NaCl, 4.75 mM KCl, 1.4 mM $CaCl_2$, 24 mM $NaHCO_3$, 1.19 mM $MgSO_4$, 1.21 mM KH_2PO_4, 11 mM glucose). The resulting solution was administered to rats *via* a catheter inserted into the right femoral vein, immediately followed by 0.2 ml of Krebs buffer alone to flush the venous catheter. An additional catheter was inserted into the right femoral artery to monitor mean arterial BP (MABP) as described previously (Supplemental Data) (41).

Data and statistical analysis

Values are expressed as means ± SEM. Data from binding studies and cAMP and AVP experiments were analyzed with GraphPad Prism (GraphPad Software, La Jolla, CA, USA). Statistical comparisons for *in vitro* assays were performed with unpaired Student's *t* test. Statistical comparisons for *ex vivo* and *in vivo* experiments were performed with 1-way ANOVA or ANOVA for repeated measures, followed by Bonferroni's *post hoc* test or Fisher's protected least significant difference test, as appropriate. Values of $P < 0.05$ were considered statistically significant.

RESULTS

Design and synthesis of metabolically stable apelin peptides

We used two strategies to protect K17F from enzymatic degradation *in vivo*. The first was a classic approach in which each amino acid was replaced by its D-isomer or an unnatural amino acid and building of structure-activity relationships. The second strategy has never been described before and represents a useful alternative to existing methods (36). It is based on the supramolecular polymerization of FCs, which is an emerging process for creating noncovalent nanostructures for material applications (42). We added FCs to the N-terminal part of K17F to constrain self-organization of the peptide in aqueous solution with the aim of increasing its stability and resistance to enzymatic degradation. FC-modified K17F was obtained by a classic solid-phase Fmoc/tbutyl strategy, isolated by reverse-phase HPLC, and fully characterized by liquid chromatography-mass spectrometry and HRMS.

Binding affinity of pE13F, K17F, and apelin analogs for rat ApelinR

As the sequence of K17F includes that of pE13F, we therefore first investigated which of the pE13F amino acids could be replaced without affecting its affinity (K_i) for ApelinR (Supplemental Table 1). Replacement in pE13F of Arg^2, Arg^4, Leu^5, Ser^6, His^7, Lys^8, Gly^9, and Phe^{13} with the corresponding D-amino acids significantly decreased affinity of the modified pE13F analogs for ApelinR by a factor 6–67 relative to pE13F (K_i = 0.56 ± 0.07 nM). The strongest effects were observed with D-Arg^2, D-Arg^4, and D-Ser^6 substitutions. By contrast, elimination of pGlu from

TABLE 2. *Pharmacologic characterization of metabolically stable apelin analogs*

Apelin analog	Binding affinity, K_i (nM)	Inhibition of FSK-induced cAMP production, IC_{50} (nM)	Internalization, EC_{50} (nM)	Recruitment of β-arrestin 2 by BRET, EC_{50} (nM)	ERK1/2 phosphorylation, EC_{50} (nM)	Half-life in plasma (min)
pE13F	0.56 ± 0.07	1.68 ± 0.47	2.50 ± 2.20	300 ± 182	12.01 ± 2.79	7.2
P26	2.11 ± 0.40	2.22 ± 1.00	2.11 ± 1.14	138 ± 30	72.10 ± 19.60	86
K17F	0.06 ± 0.01	0.30 ± 0.10	0.26 ± 0.09	15 ± 3.6	4.08 ± 1.17	4.6
P92	0.09 ± 0.02	0.56 ± 0.32	0.38 ± 0.11	4 ± 2.4	3.42 ± 2.41	24
LIT01-196	0.08 ± 0.01	1.71 ± 0.28	0.41 ± 0.16	16 ± 5.6	0.89 ± 0.61	1440

Binding affinity values (K_i), inhibitory potency (IC_{50}) of forskolin (FSK)-induced cAMP production, internalization potency (EC_{50}), recruitement of β-arrestine 2, and ERK1/2 phosphorylation capacity of the peptides represent means ± SEM from at least 3 independent experiments performed in duplicate or triplicate.

the N-terminal part of pE13F as well as the subsequent acetylation of Arg^2 or the replacement in pE13F of His^7 with α-aminoisobutyric acid (Aib), Met^{11} with norleucine (Nleu), or Phe^{13} with 4-bromo-phenylalanine (4Br-Phe) had no effect on, or slightly improved, the affinity of these compounds. We therefore combined these substitutions in pE13F to generate P26, which had a K_i value of 2.11 ± 0.40 nM (Tables 1 and **2**). Supplemental Table 2 summarizes the K_i values for the combination of substitutions in K17F. The combination in K17F of Lys^1 acetylation with the substitutions introduced in P26 resulted in the compound, P96, which has an affinity of 0.19 ± 0.10 nM. Addition of the D-Gln^5 substitution in P96 further improved affinity of the resulting compound, P95 (0.03 ± 0.02 nM), over that for K17F (K_i = 0.06 ± 0.01 nM) by a factor of 2. Finally, addition of a D-Arg substitution in position 3 in P95 gave rise to P92, which had an affinity of 0.09 ± 0.02 nM, which is similar to that of K17F. Moreover, perfluoroalkylation of the N-terminal Lys^1 residue of K17F to generate the compound, LIT01-196, did not significantly change its affinity (K_i = 0.08 ± 0.01 nM), which remained similar to that of K17F (Tables 1 and 2).

Effects of pE13F, K17F, and apelin analogs on forskolin-induced cAMP production

We incubated CHO cells that stably expressed rat ApelinR-EGFP with 5 μM forskolin in the presence of increasing concentrations of pE13F, K17F, and their analogs (10 fM to 1 μM). A concentration-dependent inhibition of forskolin-induced cAMP production was observed (Table 1 and Supplemental Tables 1 and 2).

IC_{50} values for pE13F and K17F were 1.68 ± 0.47 and 0.30 ± 0.20 nM, respectively, which were similar to those previously reported (6, 39). As shown in Supplemental Table 1, replacement of the Arg^2, Arg^4, Leu^5, Ser^6, His^7, Lys^8, Gly^9, and Phe^{13} residues of pE13F with corresponding D-amino acids greatly decreased the ability of these compounds to inhibit forskolin-induced cAMP production by a factor 25–927. By contrast, removal of pGlu from the N-terminal part of pE13F as well as the subsequent acetylation of Arg^2 or the replacement of His^7 with Aib, Met^{11} with Nleu, or Phe^{13} with 4Br-Phe had no effect on, or slightly improved, the ability of the resulting compounds to inhibit forskolin-induced cAMP production. P26 (Table 1) had an IC_{50} value (2.22 ± 1.0 nM) that is similar to that of pE13F (Table 2). P92, P95, and P96 had IC_{50} values of 0.56, 0.34, and 0.45 nmol, respectively, similar to that of K17F (0.3 nM) (Supplemental Table 2). Moreover, LIT01-196 had an IC_{50} value of 1.71 ± 0.28 nM (Table 2), which demonstrates its slightly weaker ability to inhibit forskolin-induced cAMP production (by a factor of 6) relative to K17F.

Ability of pE13F, K17F, and apelin analogs to trigger apelin receptor internalization

Confocal microscopy analysis of CHO cells that stably expressed rat apelinR-EGFP incubated with increasing concentrations of pE13F or K17F for 20 min showed progressive, marked endocytosis of ApelinR, as demonstrated by the disappearance of fluorescence at the plasma membrane and the appearance of numerous fluorescent intracellular vesicles with EC_{50} values of 2.50 ± 2.20 and 0.26 ± 0.09 nM, respectively (Table 1 and **Fig. 1**), as previously described (6). By contrast, incubation of CHO cells that stably expressed rat ApelinR-EGFP with 1 or 10 μM [D-Arg^2]pE13F, [D-Arg^4]pE13F, and [D-Lys^8]pE13F did not induce the internalization of ApelinR (Supplemental Table 1). Indeed, CHO cells displayed intense ApelinR-EGFP fluorescence at the plasma membrane, with no fluorescent intracellular vesicles. By contrast, analogs AcR12F, [Aib^7]pE13F, [D-Ala^9]pE13F, [Nle^{11}]pE13F, [4Br-Phe^{13}]pE13F, P95, and P96 strongly induced ApelinR-EGFP internalization (Supplemental Tables 1 and 2). Similarly, P26, P92, and LIT01-196 induced internalization of ApelinR, with EC_{50} values of 2.11 ± 1.14, 0.38 ± 0.11, and 0.41 ± 0.16 nM, respectively (Table 2 and Fig. 1).

Ability of pE13F, K17F, and apelin analogs to trigger β-arrestin 2 recruitment by rat apelinR

CHO cells that transiently expressed rat ApelinR that was labeled with YFP at its C terminus and *R*Luc8-β-arrestin 2 were incubated with increasing concentrations of pE13F, K17F, P26, P92, and LIT01-196 for 15 min, and BRET was monitored. For each peptide, an increase in BRET signal that corresponded to a dose-dependent recruitment of β-arrestin 2 to rat ApelinR was observed (**Fig. 2**). pE13F

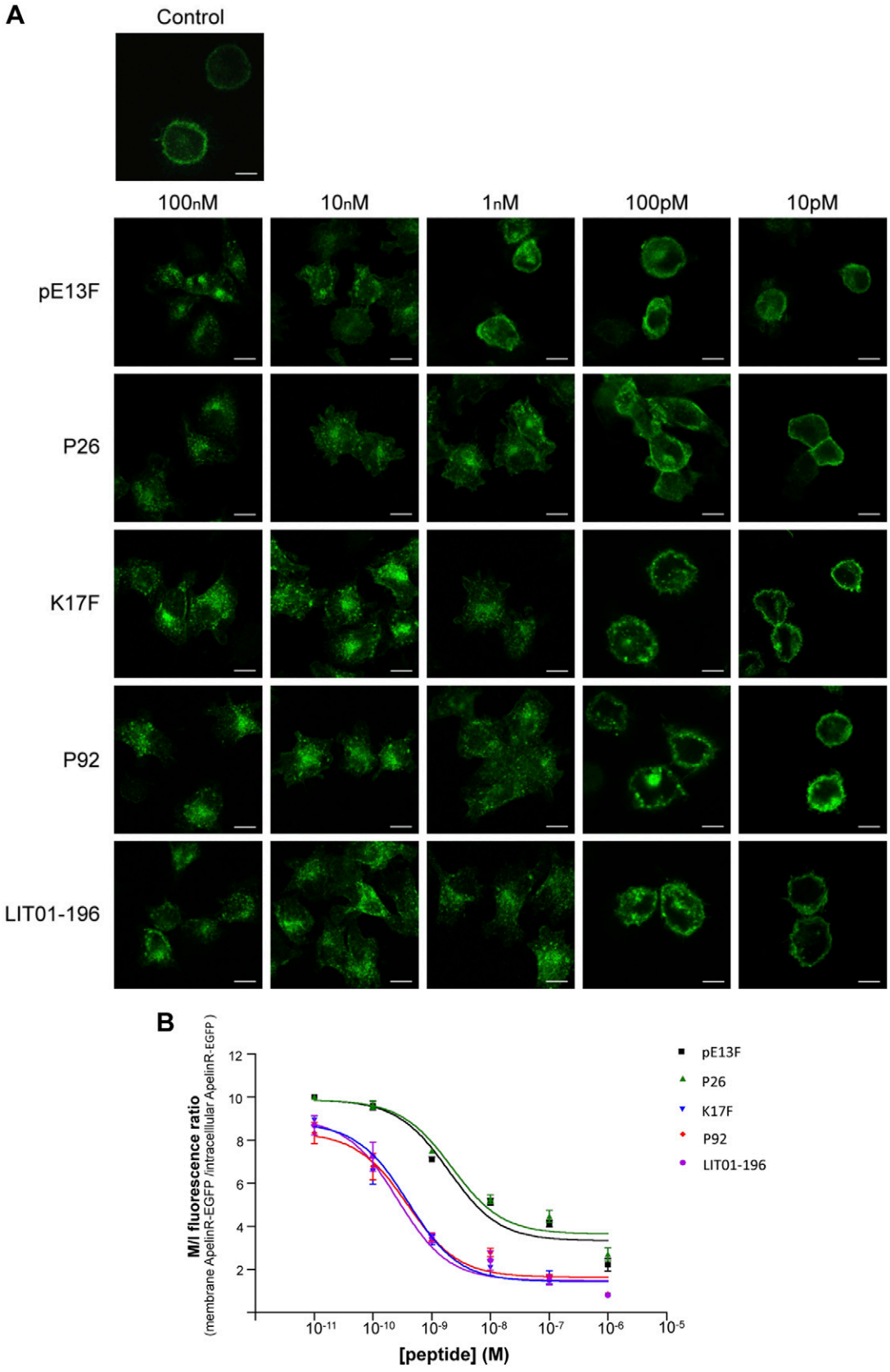

Figure 1. Effects of pE13F, P26, K17F, P92, and LIT01-196 on rat ApelinR-EGFP internalization in CHO cells. *A*) The ability of pE13F, P26, K17F, P92, K17F, and LIT01-196 to induce ApelinR internalization was evaluated in CHO cells that stably expressed rat ApelinR-EGFP that were treated with various concentrations of the compounds tested (from 10 pM to 100 nM) for 20 min at 37°C. Cells were then fixed and analyzed by confocal microscopy. Images show representative data from at least 3 independent experiments. Scale bars, 5 μm. *B*) Dose-response curves of membrane/internalized fluorescence ratio (M/I) as a function of pE13F, P26, K17F, P92, and LIT01-196 concentrations (from 10 pM to 1 μM).

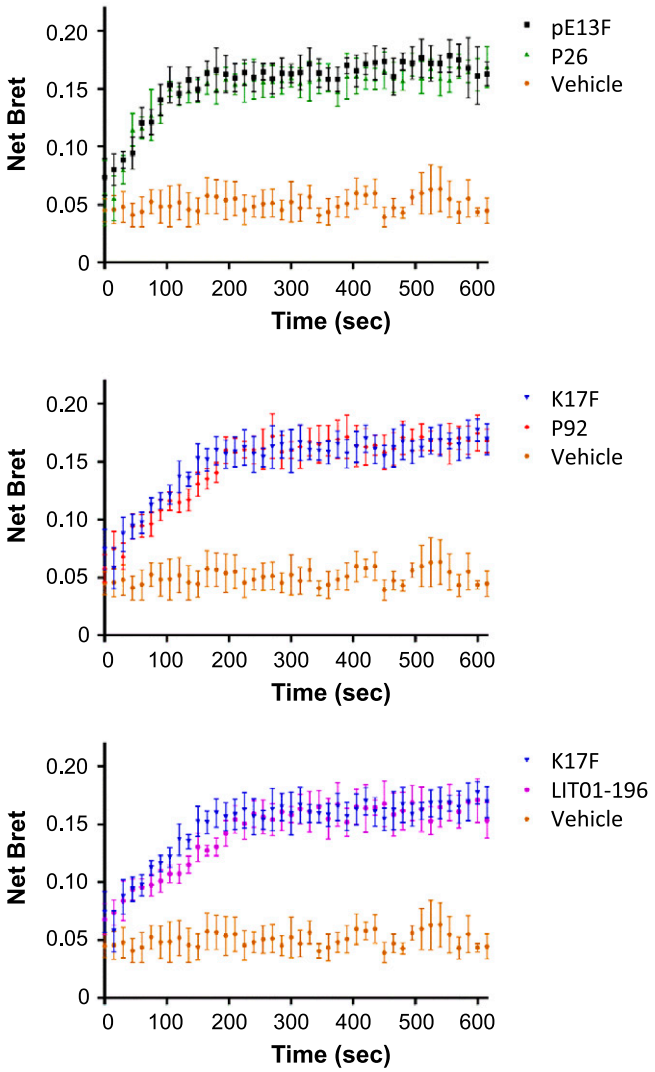

Figure 2. β-Arrestin 2 recruitment by ApelinR induced by pE13F, P26, K17F, P92, and LIT01-196 monitored by BRET1 assay. Kinetic of β-arrestin 2 recruitment induced by pE13F, P26, K17F, P92, and LIT01-196 at 10 μM. CHO cells transfected with rat ApelinR-YFP (1.6 μg) and RLuc8–β-arrestin 2 (0.8 μg) were treated with 10 μM of peptides for 15 min. Data are expressed in netBRET and correspond to means ± SE from 6 independent experiments.

and P26 were of similar potency, with EC_{50} values of 130 ± 95 and 138 ± 30 nM, respectively (Table 2). By contrast, K17F, P92, and LIT01-196 had a greater ability to recruit β-arrestin 2 (15 ± 3.6, 4 ± 2.4, and 16 ± 5.6 nM, respectively) than did pE13F and P26 (Table 2). Time-course studies of β-arrestin 2 recruitment induced by these compounds showed a rapid, strong increase in BRET signal for each peptide, with similar recruitment kinetics and maximal BRET responses (Fig. 2).

Ability of pE13F, K17F, and apelin analogs to trigger ERK1/2 phosphorylation

We assessed the ability of pE13F, K17F, and apelin analogs to induce ERK1/2 phosphorylation by stimulating CHO cells that stably expressed rat ApelinR with pE13F, K17F, P92, or LIT01-196 (1 μM) and P26 (10 μM) for up to 20 min (**Fig. 3*A***) or with increasing concentrations of the peptides (from 10 pM to 10 μM) for 10 min (Fig. 3*B*). Treatment with K17F or pE13F (1 μM) led to ERK1/2 phosphorylation,

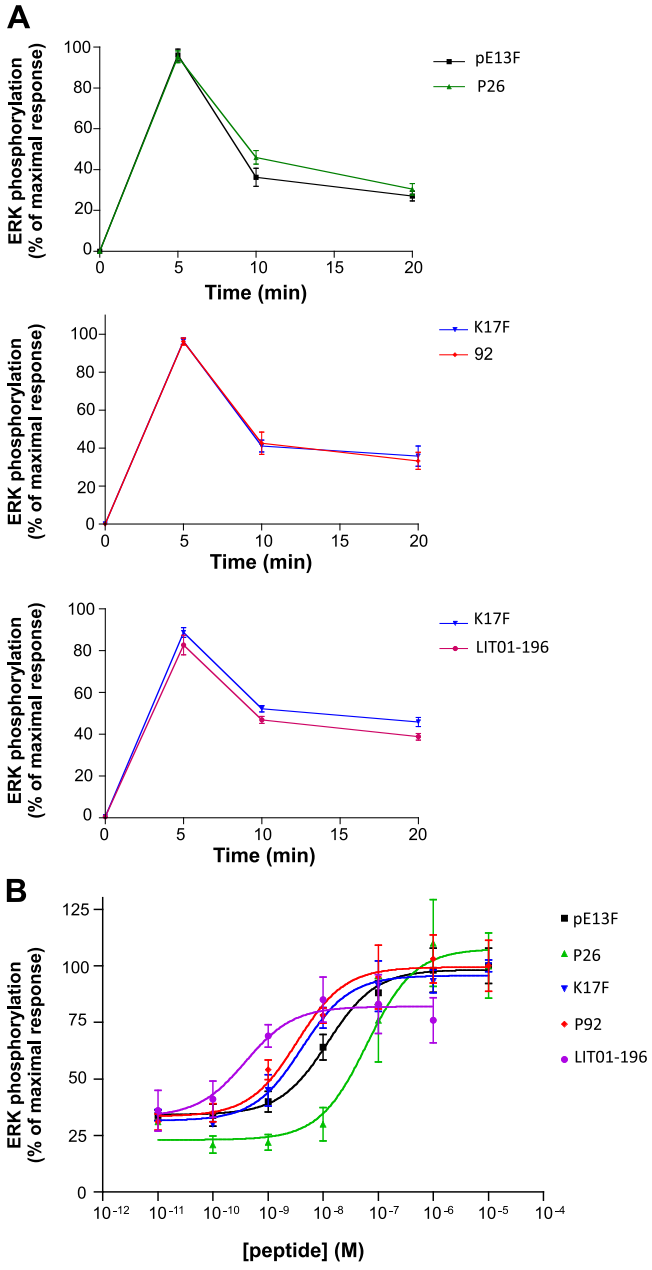

Figure 3. ApelinR-mediated ERK1/2 phosphorylation induced by pE13F, P26, K17F, P92, and LIT01-196. *A*) Time-course of ApelinR-mediated ERK1/2 phosphorylation induced by pE13F, K17F, P92, and LIT01-196 at a concentration of 1 μM or by P26 at a concentration of 10 μM. CHO cells that stably expressed Apelin R were treated with peptides for 20 min. ERK1/2 phosphorylation was assessed in an Alphascreen Surefire ERK1/2 assay. Data shown are means ± SEM from at least 3 independent experiments. *B*) Dose-response curves for induction of ERK1/2 phosphorylation by pE13F, P26, K17F, P92, and LIT01-196. Cells were treated with various concentrations (10 pM to 10 μM) of the different peptides for 10 min and ERK1/2 phosphorylation was measured in the Alphascreen Surefire ERK1/2 assay. Data shown are means ± SEM from 3–5 independent experiments.

with a maximal effect at 5 min and a plateau after 10–20 min (Fig. 3*A*). Similar time-course profiles were obtained with P26, P92, and LIT01-196 treatments. Dose-response curves for ERK1/2 phosphorylation obtained with pE13F, P26, K17F, P92, and LIT01-196 (Fig. 3*B*) showed similar maximal effects with E_{max} values (expressed in % of maximal responses) of 96 ± 7, 112 ± 17, 100 ± 3, 98 ± 10, and 87 ± 22, respectively, with no significant difference between E_{max} values. EC_{50} values for K17F, P92, and LIT01-196 were 4.08 ± 1.17, 3.42 ± 2.41, and 0.89 ± 0.61 nM, respectively (Table 2). By contrast, pE13F and P26 promoted ERK1/2 phosphorylation less strongly, with EC_{50} values of 12.01 ± 2.79 and 72.1 ± 19.6 nM, respectively (Table 2).

Plasma stability of pE13F, K17F, and apelin analogs

We assessed the stability of pE13F, K17F, P26, P92, and LIT01-196 in mouse plasma that was incubated at 37°C (Table 2). K17F and pE13F had half-lives in plasma of 4.6 and 7.2 min, respectively, whereas P92 and -26 (analogs of K17F and pE13F) were more stable in plasma, with half-lives of 24 and 86 min, respectively. Plasma stability was greatly increased in LIT01-196, with >90% of this compound remaining unchanged after 24 h of incubation.

Vasorelaxing effects of pE13F, K17F, and apelin analogs on isolated aorta and glomerular arterioles

K17F, P92, and LIT01-196 induced a concentration-dependent relaxation in male rat aortic rings that were precontracted with 3 μM NE (**Fig. 4*A***). K17F (8 ± 3 nM) and P92 (7 ± 5 nM) had similar EC_{50} values, with maximal relaxing effects of 94 ± 7% and 100 ± 1%, respectively. By contrast, although LIT01-196 (2 ± 1 nM) had a significantly better EC_{50} ($P < 0.05$), its maximal vasorelaxing effect induced by 100 μM LIT01-196 (60 ± 3%) was significantly weaker than that of K17F (94 ± 7%, $P < 0.01$; Fig. 4*A*). The vasorelaxant effects of 0.1 and 1 μM K17F (61 ± 4% and 79 ± 5%, respectively), P92 (67 ± 10% and 89 ± 7%, respectively), and LIT01-196 (45 ± 3% and 50 ± 3%, respectively) were significantly inhibited in the presence of 30 μM L-NAME [N(G)-nitro-L-arginine methyl ester], a NO synthase inhibitor (12 ± 13% and 13 ± 14%, respectively, for K17F; 26 ± 6% and 38 ± 9%, respectively, for P92; 19 ± 3% and 22 ± 4%, respectively, for LIT01-196; $P < 0.001$).

Male rat glomerular arterioles that were precontracted with 1 nM AngII had a significantly smaller diameter than did those in baseline conditions (14.30 ± 0.33 *vs.* 12.97 ± 0.50 μm; $n = 5$; $P < 0.01$, respectively). Addition of 500 nM P92 to these arterioles increased their diameter from 12.97 ± 0.50 to 14.32 ± 0.33 μm ($n = 5$; $P < 0.01$), a value similar to that obtained in the presence of 500 nM K17F, which triggered an increase from 12.97 ± 0.50 to 14.27 ± 0.39 μm ($n = 5$; $P < 0.01$; Fig. 4*B*). Moreover, addition of 500 nM LIT01-196 to precontracted arterioles with 1 nM AngII increased their diameter from 12.97 ± 0.50 to 13.88 ± 0.45 μm ($n = 5$; $P < 0.05$).

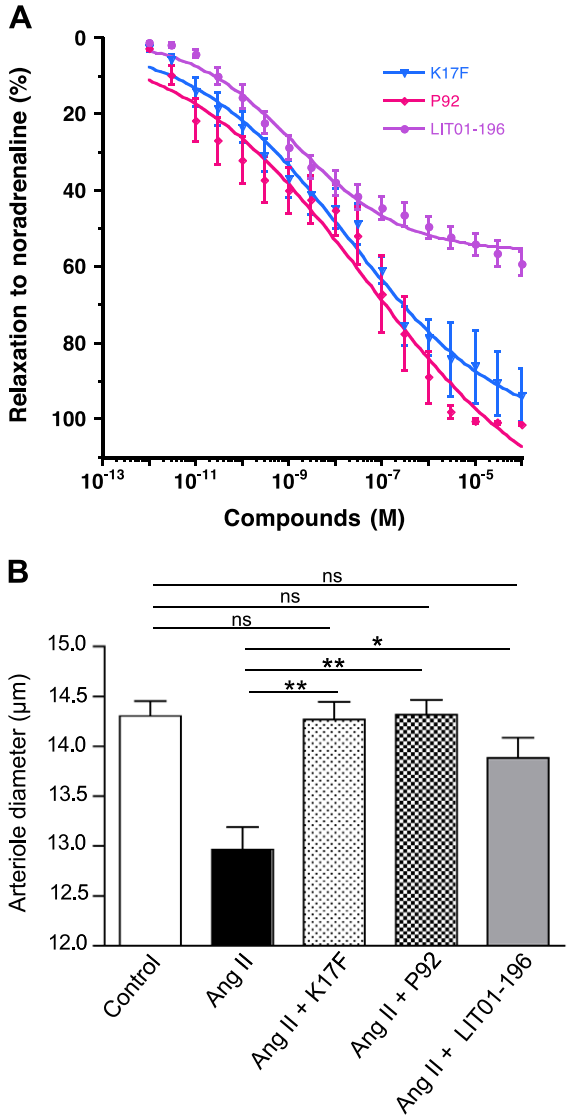

Figure 4. Vasorelaxant effects of K17F and apelin analogs. *A*) Cumulative concentration-response curves for K17F (blue), P92 (red), and LIT01-196 (purple) in rat aorta that were precontracted by incubation with NE (3 μM). *B*) Effects of K17F, P92, and LIT01-196 on the rat glomerular arteriole contractile response to 1 nM AngII. Arteriolar diameters were measured under basal conditions (control), then 1 min after addition of AngII (1 nM) and 1 min after addition of 500 nM K17F, P92, or LIT01-196 to the arterioles that displayed AngII-induced vasoconstriction. Data shown are means ± SEM for 5–8 independent experiments. ns, not significant. *$P < 0.05$; **$P < 0.01$.

Effects of K17F and P92 on cardiac contractility in isolated perfused rat heart preparations

After a 20-min equilibration period, hearts from male rats were treated by perfusion with the various compounds at a constant flow rate. For all experimental groups, baseline values were similar for heart rate (320 ± 16 bpm),

perfusion pressure (41.8 ± 3.2 mmHg), systolic pressure (65.2 ± 3.0 mmHg), and dP/dt_{max} (3717 ± 81 mmHg/s), with no significant difference between groups. We compensated for the possible effect of a change in heart rate on left ventricular pressure by evaluating cardiac contractility by determining rate-pressure product (the product of heart rate and left ventricular dP). K17F (1–300 nM) increased rate-pressure product in a dose-dependent manner, with EC_{50} 28 ± 1.5 nM (Supplemental Fig. 2). We then compared the effects of K17F and P92 at a supramaximal concentration (100–400 nM) on the maximum increase in left ventricular pressure (dP/dt_{max}). The increase in heart contractility induced by K17F or P92 was gradual: dP/dt_{max} began to increase within 15 min and was still increasing 30 min after the start of the perfusion (**Fig. 5**). K17F (100 nM) induced the largest increase in dP/dt_{max}: +7.72 ± 1.23% *vs.* −2.99 ± 2.57% in the control group ($P < 0.01$; Fig. 5). Similarly, P92 increased dP/dt_{max} when administered at concentrations of 200 nM/L (+6.93 ± 0.88%; $P < 0.01$) or 400 nM (+8.00 ± 1.59%; $P < 0.01$; Fig. 5).

Effects of intracerebroventricular injection of P92 and LIT01-196 on systemic vasopressin release in conscious mice deprived of water for 24 h

Water deprivation for 24 h significantly increased plasma AVP levels in mice in 2 sets of experiments (425 ± 46 pg/ml; $n = 18$ *vs.* control mice 175 ± 17 pg/ml; $n = 20$; $P < 0.001$; **Fig. 6*A***; and 644 ± 60 pg/ml; $n = 14$ *vs.* control mice 232 ± 54 pg/ml; $n = 8$; $P < 0.001$; Fig. 6*B*). As previously described (6), intracerebroventricular injection of 1 μg (468 pmol) K17F into water-deprived mice resulted in significantly lower plasma AVP levels (190 ± 27 pg/ml; $n = 7$) than did injection of saline (425 ± 46 pg/ml) into water-deprived mice ($P < 0.001$; Fig. 6*A*). The intracerebroventricular injection of P92 (at doses of 0.01–1 μg, corresponding to 4.5–454 pmol) into water-deprived mice induced a dose-dependent decrease in plasma AVP levels. ED_{50} for P92 (0.02 μg = 9.1 pmol; Fig. 6*A*, inset) was lower than that of K17F by a factor of 6 (ED_{50} = 56 pmol) (6). The maximal decrease in AVP release induced by P92 (85% decrease) at a dose of 0.1 μg (45 pmol/mouse) was similar to that observed with 1 μg (468 pmol/mouse) K17F (94% decrease; Fig. 6*A*). The intracerebroventricular injection of LIT01-196 (0.0001–1 μg, corresponding to 0.029–293 pmol) into water-deprived mice triggered a dose-dependent decrease in plasma AVP levels (Fig. 6*B*). The maximal decrease in AVP release induced by LIT01-196 was observed for doses between 0.01 and 1 μg (2.93–293 pmol/mouse) LIT01-196 (78% decrease). ED_{50} for LIT01-196 (0.0012 μg = 0.35 pmol; Fig. 6*B*, inset) was lower than that of K17F by a factor of 160. Moreover, intracerebroventricular injection of P92 and LIT01-196 alone into normally hydrated mice at a supramaximal dose of 1 μg had no effect on plasma AVP levels.

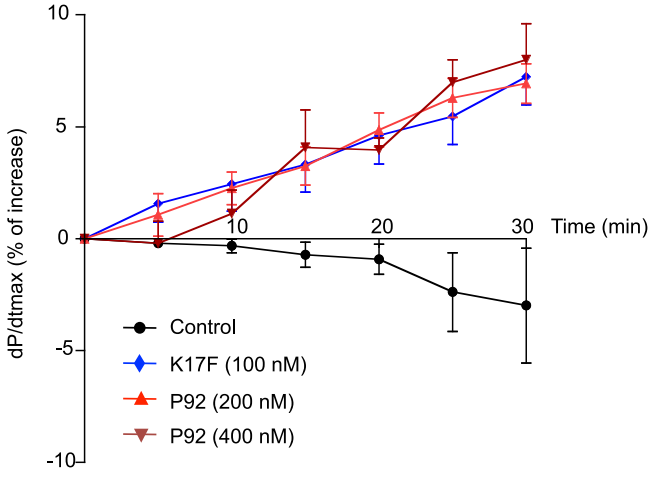

Figure 5. Effects of K17F and P92 on cardiac contractility in isolated perfused rat heart preparations. Left ventricular pressure was recorded in isolated rat heart after administration of K17F (100 nM), P92 (200 and 400 nM) or vehicle (control). Data shown are means ± SEM ($n = 8$).

Effects of intravenous injection of P92 on diuresis in anesthetized rats

Intravenous injection of K17F at a dose in the nmol/kg range in anesthetized lactating rats was previously shown to increase diuresis rate (14, 43). In this study, diuresis rate measured in anesthetized virgin rats ($n = 10$) during the 2-h control period was 2.5 ± 0.4 μl/min/100 g (Fig. 6*C*). The intravenous injection of P92 (5 nmol/rat = 20 nmol/kg = 44 μg/kg) resulted in a 116% increase in diuresis rate measured during the 2 h that followed injection (5.4 ± 0.6 μl/min/100 g; $n = 5$). In comparison, intravenous injection of saline resulted in a nonsignificant 12% increase in diuresis rate (2.8 ± 0.3 μl/min/100 g; $n = 5$; Fig. 6*C*).

Effects of intravenous injection of K17F, P92, and LIT01-196 on arterial BP in anesthetized normotensive rats

Basal MABP was 100.3 ± 1.2 mmHg in anesthetized normotensive Wistar rats. The intravenous injection of K17F (15 nmol/rat = 50 nmol/kg = 0.106 mg/kg) decreased MABP by 5.4 ± 1 mmHg (**Fig. 7*A***). Mean hypotensive response was maximal 1.2 ± 0.1 min after injection and was transient, which reflected the rapid enzymatic degradation of the peptide in the bloodstream. A return to baseline (0.8 ± 2.4 mmHg) was observed 4 ± 0.7 min after injection. At a dose of 15 nmol/rat (0.11 mg/kg), P92 was much more effective than K17F, reducing MABP by −18.6 ± 3.4 mmHg (Fig. 7*A*; in 1.3 ± 0.3 min, $P < 0.05$ *vs.* Wistar rats receiving 15 nmol K17F), with a return to baseline values (−4.0 ± 1.2 mmHg) by 14 min. The intravenous injection of K17F (100 nmol/rat = 0.71 mg/kg) caused a maximum decrease in MABP of 25.6 ± 8.4 mmHg at 2.7 min after injection, with a return to the plateau value (−10 ± 2.4 mmHg) by 35 min (Supplemental Fig. 2*B*). For P92 at the same dose (100 nmol/rat or 0.73 mg/kg), we observed a maximum decrease in MABP of 46.2 ± 5.8 mmHg, with a return to a value of −18.7 ± 2.9 mmHg by 35 min (Supplemental Fig. 2*B*). In anesthetized Wistar rats, intravenous injection of P92 or K17F (5–100 nmol/rat)

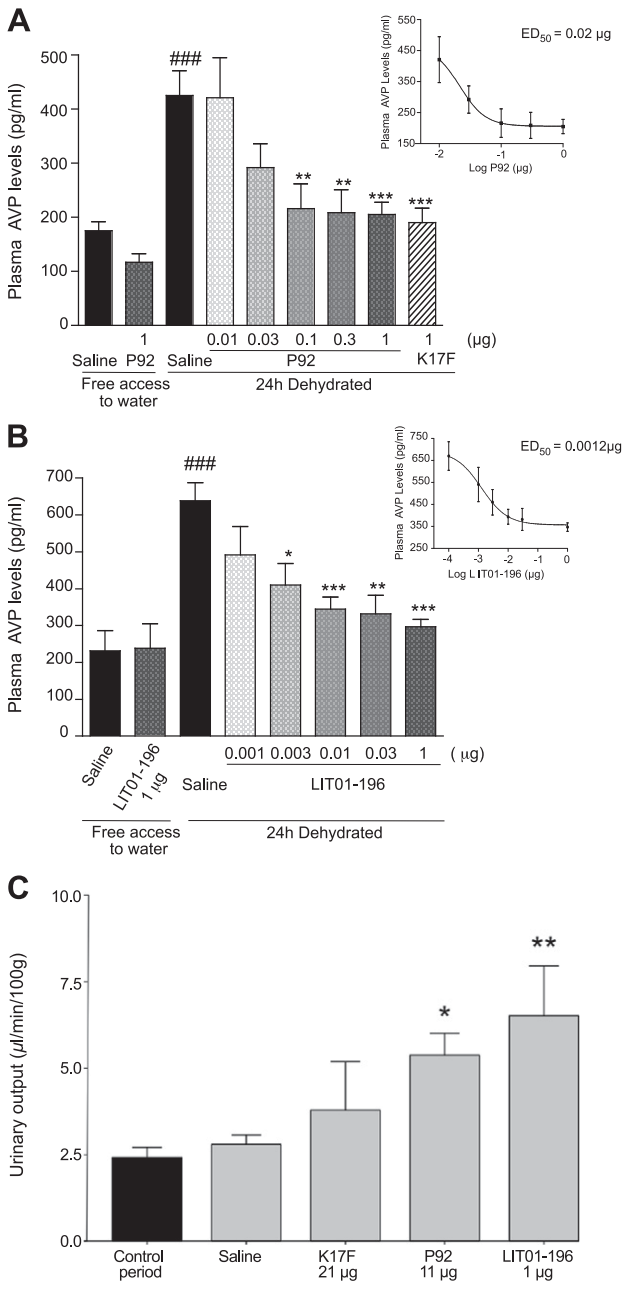

Figure 6. Effects of K17F, P92, and LIT01-196 systemic AVP release in water-deprived mice and on diuresis in anesthetized rats. *A*, *B*) After 24 h of water deprivation, mice received 10 µl saline or various amounts of P92 (0.01–1 µg), K17F (1 µg) (*A*) or LIT01-196 (0.0001–1 µg) (*B*) *via* intracerebroventricular route and were compared with mice that were given free access to water and that received 10 µl saline, P92 (1 µg), or LIT01-196 (1 µg) *via* intracerebroventricular route. Plasma AVP levels were determined 1 min after injection by radioimmunoassay. Histograms show means ± SEM for plasma AVP levels (pg/ml) from 7 to 20 animals for each set of conditions. Sigmoidal curves of dose responses for AVP release in response to P92 or LIT01-196 in conscious water-deprived mice (insets). $^{###}P < 0.001$ *vs.* normally hydrated; $^{*}P < 0.05$, $^{**}P < 0.01$, $^{***}P < 0.001$ *vs.* water-deprived mice administered saline. *C*) The diuresis rate was monitored in anesthetized virgin female rats for a 2-h control period after intravenous saline injection ($n = 21$; black column) and for 2 h after intravenous injection of either saline ($n = 6$), K17F (40 nmol/kg; $n = 5$), P92 (20 nmol/kg; $n = 5$), or LIT01-196 (2 nmol/kg; $n = 5$; gray columns). Each column represents the mean diuresis rate ± SEM. * $P < 0.05$, ** $P < 0.001$ compared with control period.

decreased MABP in a dose-dependent manner, with an ED_{50} of 29.5 (0.21 mg/kg) and 30 nmol (0.22 mg/kg), respectively (Fig. 7*B*). Calculation of the area under the curve for MABP response confirmed the stronger BP-lowering effect in Wistar rats that received intravenous injections of P92 than in rats that received intravenous injections of K17F (area under the curve after 100 nmol P92 *vs.* 100 nM

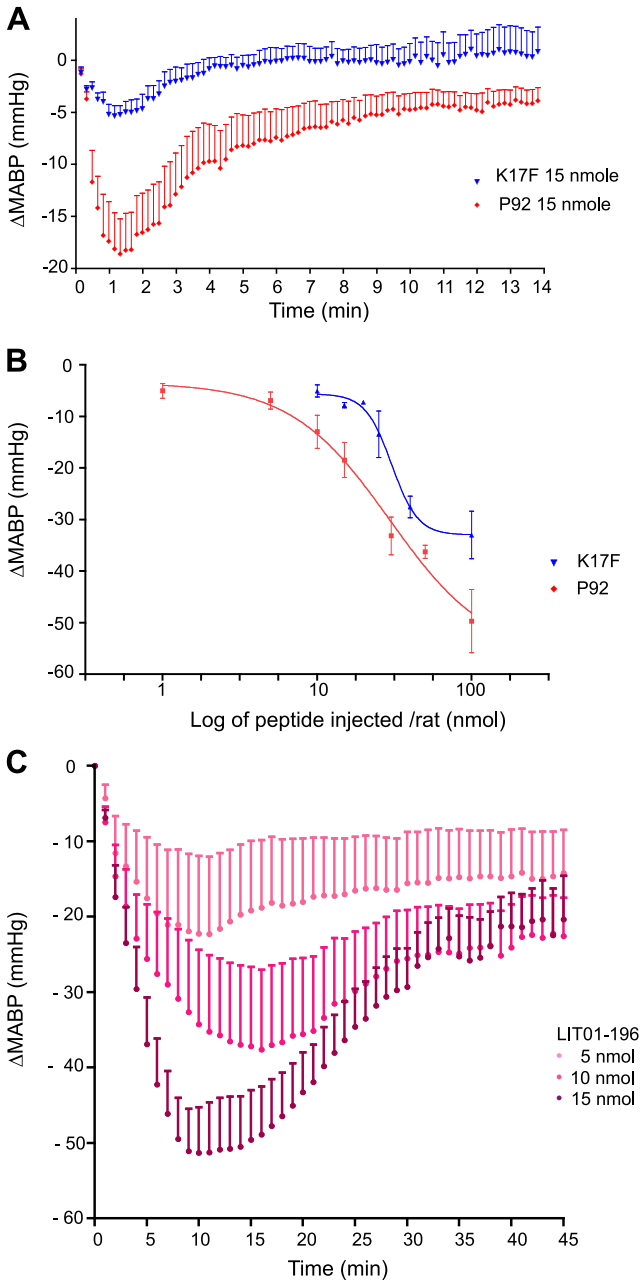

Figure 7. Effects of intravenous injection of K17F, P92, and LIT01-196 on MABP in anesthetized normotensive rats. *A*) Time course of mean ± SEM values for MABP after a single i.v. injection of 15 nmol per animal (50 nmol/kg) of K17F (0.106 mg/kg) or P92 (0.11 mg/kg) in Wistar rats. *B*) Dose-response curves for the decrease in BP induced by K17F and P92. *C*) Time course of the mean ± SEM values for MABP after a single intravenous injection of various doses of LIT01-196 (5–15 nmol/rat corresponding to 0.043–0.13 mg/kg). Data shown are means ± SEM for the animals in each set of conditions ($n = 5$–8).

K17F: −34303 ± 4003 mmHg/s *vs.* −13712 ± 5271 mmHg/s; $P < 0.05$). The intravenous injection of LIT01-196 (from 5 to 15 nmol/rat, corresponding to 0.043–0.13 mg/kg) into anesthetized Wistar rats (Fig. 7*C*) decreased MABP in a dose-dependent manner, with a maximal decrease of 51.4 ± 6.1 mmHg at 10 min for a dose of 15 nmol/rat *vs.* 5.4 ± 1 mmHg for K17F at the same dose. A slight decrease in MABP (between 6 and 10 mmHg) persisted 108 min after injection. Decrease in MABP and the duration of the BP-lowering effect at 15 nmol were 9 and 27 times larger than those observed for K17F at the same dose.

DISCUSSION

Endogenous apelin peptides have pharmacological properties of considerable potential utility for the treatment of cardiovascular diseases and body fluid disorders, but their use is limited by their short biological half-lives. Development of selective, metabolically stable ApelinR agonists is therefore required to facilitate further explorations of the role of this peptide in diseases and the design of new, more druggable compounds. Here, we identified 2 potent, metabolically stable K17F analogs: P92, generated by classic chemical substitutions in K17F, and LIT01-196, which was produced by the original and still undescribed chemical addition of a FC group onto K17F. Both compounds had a subnanomolar affinity for ApelinR, behaved as full agonists for cAMP production, ERK1/2 phosphorylation, β-arrestin recruitment, and ApelinR internalization, and were much more stable in plasma than K17F. *Ex vivo*, P92 and LIT01-196 relaxed rat aorta and glomerular arterioles that were precontracted with NE and AngII, respectively, and P92 increased cardiac contractility in isolated perfused rat heart preparations. *In vivo*, P92 and LIT01-196 strongly inhibited AVP release into the bloodstream, increased diuresis, and decreased arterial BP.

The short half-life of peptides has been one of the major issues of peptide therapeutics as they are typically cleared from the bloodstream within minutes after administration. As a result, the interaction with their specific target is too short to observe a significant *in vivo* effect. Short peptide half-lives typically result from fast renal clearance and enzymatic metabolism. Numerous technologies, such as PEGylation, conjugation to albumin, N-terminal acetylation, C-terminal amidation, use of unnatural amino acids, or main chain modifications (cyclization), have now been set up to increase the *in vivo* plasma half-life of peptides (36). Most studies that aim to develop apelin analogs have focused on pE13F (33–35); however, K17F, which had an affinity 10 times higher than that of pE13F for human ApelinR, was 10 times more efficient at inducing internalization of rat ApelinR and also decreased arterial BP more strongly than did pE13F (9). Given these findings and the short half-life of K17F (4.6 min in plasma; Table 2), we aimed to generate more potent and metabolically stable K17F analogs. We replaced each amino acid of the sequence of K17F, which includes that of pE13F, with its D-isomer or with an unnatural amino acid. Because we found—in agreement with previous alanine scanning pE13F studies (32)—that replacement of the Arg^2, Arg^4, Ser^6, Lys^8, and Gly^9 residues of pE13F with corresponding D-amino acids greatly decreased the ability of these compounds to bind to ApelinR or to inhibit forskolin-induced cAMP production, we first combined $pGlu^1$ deletion with N-acetyl Arg^2, D-Leu^5, Aib^7, D-Ala^9, Nle^{11}, and 4Br-Phe^{13} in pE13F, which generated P26 and had an affinity of 2.1 nM, whereas that of pE13F was 0.6 nM. These substitutions were then incorporated into K17F together with the acetylation of Lys^1 and the introduction of D-Arg^3 and D-Gln^5 to generate P92, which had an affinity of 0.09 nM, similar to that of K17F (0.06 nM). Our decision to introduce a Br-Phe residue into the C-terminal part of P26 or P92 was guided by previous findings. Structure-activity studies on apelin (6, 8, 9) have shown that deletion of the C-terminal Phe residue of K17F strongly decreases its ability to trigger ApelinR internalization, β-arrestin recruitment, and β-arrestin–dependent ERK1/2 phosphorylation, which, in turn, affects the ability of the apelin peptide to lower BP. These findings are consistent with those of structure-function studies that demonstrated that the C-terminal Phe residue of K17F is embedded in a hydrophobic cavity that is composed of Phe^{255} and Trp^{259} at the bottom of the ApelinR binding site. Replacement of these residues by alanine abolishes the ability of ApelinR to internalize upon K17F stimulation, which demonstrates the need for an interaction between these residues and the C-terminal Phe of K17F for ApelinR internalization (6). Finally, Murza *et al.* (44) showed that the replacement of Phe^{13} in pE13F with a (4-bromo)Phe residue had no major effect on the affinity of the new compound and its ability to inhibit cAMP production or to induce β-arrestin mobilization compared with pE13F.

We also describe here an original strategy for improving the protection of endogenous peptides against enzymatic degradation on the basis of the introduction of an FC directly into the N-terminal part of K17F to generate LIT01-196, the first FC-modified apelin peptide described to date. The presence of the FC on the apelin peptide had no impact on the affinity of LIT01-196 for ApelinR (K_i = 0.08 nM), nor on its solubility in water (>10 mM).

Altogether these chemical modifications allowed us to extend the plasma half-lives of P26 and P92 by a factor of 6–11. This was, in part, a result of the chemical modifications introduced in pE13F: D-Leu5 and 4Br-Phe13 and also in K17F, which could account for the highest resistance of P26 and P92 to proteolytic cleavage by neutral endopeptidase 24.11 (NEP, neprilysin) at the Arg^4/Leu^5 and Leu^5-Ser^6 peptide bonds and angiotensin-converting enzyme type 2 at the C-terminal Phe^{13} of pE13F. Both enzymes were indeed shown to be involved in the metabolism of native peptides pE13F and K17F (45, 46). The plasma half-life of LIT01-196 was extended by a factor of >100 relative to those of pE13F and K17F. LIT01-196 displayed remarkable resistance to degradation by plasma enzymes, as >90% of the peptide remained unchanged after 24 h of incubation at 37°C. FC acylation of an endogenous peptide therefore seems to be an efficient way to extend its half-life in plasma.

A battery of functional tests *in vitro* then identified 2 sets of compounds with greater metabolic stability. The most potent molecules in the first set were P92 and LIT01-196,

both of which had a subnanomolar affinity and displayed full agonist activity for cAMP production, ERK1/2 phosphorylation (nanomolar range), induction of ApelinR internalization (subnanomolar range), and β-arrestin recruitment. The second set included P26 and pE13F, both of which had lower levels of pharmacological activity than did the molecules of the first set.

We therefore decided to further investigate the *ex vivo* and *in vivo* potencies of P92 and LIT01-196 in biological responses known to be driven by ApelinR signaling. We first studied their vasorelaxant activity on isolated rat aorta that were precontracted by incubation with NE and on glomerular arterioles that were precontracted with AngII. In both preparations, P92 and LIT01-196, as with K17F, induced a dose-dependent relaxation of the vessels. The NO component of the relaxant effect of P92 was similar to that of K17F, which was consistent with the presence of ApelinR binding sites in human aorta (47) and of ApelinR mRNA in the endothelial cells lining the large conductance vessels of various organs (43, 48). The kinetics of the relaxant effect of LIT01-196 on rat aorta differed from those for K17F and P92. and its maximal effect was of only 60% *vs*. 94% and 100% for K17F and P92, respectively. The relaxant effects of K17F, P92, and LIT01-196 on rat aorta were significantly inhibited by prior treatment of the vessels with the NO-synthase inhibitor, N(G)-nitro-L-arginine methyl ester, which suggested that P92 and LIT01-196, similar to K17F, acted *via* a NO-dependent mechanism. As the K17F-induced BP decrease was shown to occur *via* a NO-mediated arterial vasodilation (19) and may involve the internalization of ApelinR and subsequent β-arrestin–dependent ERK1/2 activation (8), the P92- and LIT01-196–induced aorta vasodilation could be mediated by endocytosis of ApelinR as these compounds are full agonists with regard to internalization and ERK1/2 MAPK activation. We then measured the inotropic effect of P92 with Langendorff isolated rat heart preparations. We showed that the chemical modifications introduced in P92 had no effect on its ability to increase cardiac contractility, a widely documented property of apelin (49).

We then evaluated these compounds *in vivo*. The intravenous administration of P92 and LIT01-196 in normotensive anesthetized rats resulted in a dose-dependent decrease in arterial BP. The BP-lowering effect of these 2 compounds was stronger and persisted for longer than did that of K17F. Identical ED_{50} values were obtained for P92 and K17F (100 nmol/kg), but MABP returned to its baseline value after 2 min for K17F and had not fully recovered after 14 min for P92. Marked differences in potency were also observed. At a dose of 50 nmol/kg, the maximum decrease in BP, which occurred at approximately the same time after bolus injection (1.2 min), was 5 and 19 mmHg for K17F and P92, respectively. Even more marked differences were observed between LIT01-196 and K17F. For example, the maximal decrease in BP (by 51 mmHg) and the duration (>108 min) of the BP-lowering effect induced by injection of 50 nmol/kg LIT01-196 were 9 and 27 times higher, respectively, than those induced by K17F. Because the return to baseline values for K17F, P92, and LIT01-196 occurred at 4, 35, and >108 min, respectively, this suggests that the *in vivo* half-lives of K17F, P92, and LIT01-196 should be approximately 1–2, 15, and >50 min, respectively. In comparisons with the most potent apelin 13 analog, compound 12, that has been previously reported (35), in which Phe^{13} was replaced with P-$Tyr(OBn)^{13}$ and Met^{11} with Nle, and that had a subnanomolar affinity for ApelinR and an *ex vivo* plasma half-life of 66 min, P92 and LIT01-196 were found to have greater BP-lowering activities *in vivo*. Indeed, the decrease in MABP induced by intravenous administration of 12 (0.1 mg/kg or 61 nmol/kg) to anesthetized normotensive rats was intense between 0 and 2 min (decreases of 30–40 mmHg), but returned to near-basal levels (−10 mmHg) after 6 min, highlighting the difference between the duration of action of a compound in plasma and *in vivo*. The high efficiency of LIT01-196 in decreasing BP after a single administration to normotensive animals requires an investigation of its antihypertensive activity in various experimental models of hypertension. Moreover, the decrease in vascular resistance induced by these compounds—resulting in decreases in cardiac afterload and preload, together with their positive inotropic action—make them suitable candidates for use in HF treatment. They could help to improve the mechanical efficiency of dilated hearts and to reduce ventricular wall stress and oxygen demands in failing hearts. Consistent with this hypothesis, a beneficial effect of apelin infusion was observed in humans with chronic HF (27).

We also investigated whether the central administration of P92 or LIT01-196, as with that of apelin, could decrease systemic AVP release in mice that are deprived of water for 24 h. P92 and LIT01-196 decreased dehydration-induced AVP release in a dose-dependent manner, and they were 6 and 160 times, respectively, more effective than K17F. These data suggest that P92 and LIT01-196, like K17F, rapidly reach the hypothalamic structures that are involved in AVP release from the posterior pituitary into the bloodstream after intracerebroventricular injection. They subsequently act on ApelinR expressed by AVP neurons to inhibit their phasic electrical activity, thereby preventing AVP release into the bloodstream (3). Furthermore, intravenous administration of P92 in anesthetized rats, at a dose in the nmol/kg range, potently increased urine output. In parallel, the vasorelaxation of juxtamedullary arterioles, which gives rise to vasa recta, by P92 or LIT01-196 strongly suggests that these apelin analogs can act like K17F to increase medullary blood flow (43). Thus, by decreasing AVP release into the bloodstream and by increasing both renal blood flow and urine output, these new compounds should also have an aquaretic effect similar to that previously reported for K17F in lactating rats (3, 43). ApelinR agonists of this type would be particularly useful for the treatment of water retention and hyponatremia, making it possible to avoid the excessive sodium loss that is frequently reported in patients receiving thiazidic diuretics.

In summary, addition of an FC to K17F to generate LIT01-196 constitutes an efficient, novel strategy for protecting K17F against *in vivo* enzymatic degradation without changing its affinity. This approach could potentially be extended to other endogenous peptides. Moreover, the chemical modifications used to generate P92 and

LIT01-196 resulted in compounds with a subnanomolar affinity and *in vitro* pharmacological profiles similar to that of K17F, but with much longer plasma half-lives and greater *in vivo* activity. The efficacy of these lead compounds for decreasing AVP release and increasing both renal blood flow and diuresis, as well as their ability to decrease BP and improve cardiac function make them promising candidates for the treatment of HF, water retention, and/or hyponatremic disorders. FJ

ACKNOWLEDGMENTS

The authors thank Julie Sapa for the editing the article, Jérémie Teillon (Center for Interdisciplinary Research in Biology for Microscopy Core Facility), Patrick Gizzi (TechMedILL Platform, Illkirch, France), and Nicolas Humbert and Hugues de Rocquigny (Laboratory of Biophotonics and Pharmacology, Illkirch, France) for peptides synthesis. This work was supported by INSERM (through financial support for Proof of Concept, CoPoC, in particular), the Centre National de la Recherche Scientifique, the Université de Strasbourg, the Collège de France, and the Agence Nationale pour la Recherche "Physique et Chimie du Vivant 2009." R.G., J.G., E.C., and L.E were supported by fellowships from "Cardiovasculaire-Obésité-Rein-Diabète" (Région Ile-de-France), Fondation Lefoulon-Delalande, and the French "Ministère de l'Education Nationale, de l'Enseignement Supérieur et de la Recherche."

AUTHOR CONTRIBUTIONS

R. Gerbier designed the studies, conducted experiments, acquired and analyzed data, and wrote the manuscript; R. Alvear-Perez, J.-F. Margathe, A. Flahault, P. Couvineau, J. Gao, H. Dabire, B. Li, E. Ceraudo, and A. Hus-Citharel participated in the design of the studies, conducted experiments, and performed data analysis; N. De Mota, L. Esteoulle, and C. Bisoo conducted experiments; M. Hibert and A. Berdeaux participated in the design of the studies and revised the manuscript; X. Iturrioz and D. Bonnet coordinated the *in vitro* pharmacological and chemical studies and wrote the manuscript; and C. Llorens-Cortes supervised the work, participated in the study design and analysis, and wrote the manuscript.

REFERENCES

1. O'Dowd, B. F., Heiber, M., Chan, A., Heng, H. H., Tsui, L. C., Kennedy, J. L., Shi, X., Petronis, A., George, S. R., and Nguyen, T. (1993) A human gene that shows identity with the gene encoding the angiotensin receptor is located on chromosome 11. *Gene* **136**, 355–360
2. Tatemoto, K., Hosoya, M., Habata, Y., Fujii, R., Kakegawa, T., Zou, M. X., Kawamata, Y., Fukusumi, S., Hinuma, S., Kitada, C., Kurokawa, T., Onda, H., and Fujino, M. (1998) Isolation and characterization of a novel endogenous peptide ligand for the human APJ receptor. *Biochem. Biophys. Res. Commun.* **251**, 471–476
3. De Mota, N., Reaux-Le Goazigo, A., El Messari, S., Chartrel, N., Roesch, D., Dujardin, C., Kordon, C., Vaudry, H., Moos, F., and Llorens-Cortes, C. (2004) Apelin, a potent diuretic neuropeptide counteracting vasopressin actions through inhibition of vasopressin neuron activity and vasopressin release. *Proc. Natl. Acad. Sci. USA* **101**, 10464–10469
4. Habata, Y., Fujii, R., Hosoya, M., Fukusumi, S., Kawamata, Y., Hinuma, S., Kitada, C., Nishizawa, N., Murosaki, S., Kurokawa, T., Onda, H., Tatemoto, K., and Fujino, M. (1999) Apelin, the natural ligand of the orphan receptor APJ, is abundantly secreted in the colostrum. *Biochim. Biophys. Acta* **1452**, 25–35
5. De Mota, N., Lenkei, Z., and Llorens-Cortès, C. (2000) Cloning, pharmacological characterization and brain distribution of the rat apelin receptor. *Neuroendocrinology* **72**, 400–407
6. Iturrioz, X., Alvear-Perez, R., De Mota, N., Franchet, C., Guillier, F., Leroux, V., Dabire, H., Le Jouan, M., Chabane, H., Gerbier, R., Bonnet, D., Berdeaux, A., Maigret, B., Galzi, J. L., Hibert, M., and Llorens-Cortes, C. (2010) Identification and pharmacological properties of E339-3D6, the first nonpeptidic apelin receptor agonist. *FASEB J.* **24**, 1506–1517
7. Masri, B., Morin, N., Cornu, M., Knibiehler, B., and Audigier, Y. (2004) Apelin (65-77) activates p70 S6 kinase and is mitogenic for umbilical endothelial cells. *FASEB J.* **18**, 1909–1911
8. Ceraudo, E., Galanth, C., Carpentier, E., Banegas-Font, I., Schonegge, A. M., Alvear-Perez, R., Iturrioz, X., Bouvier, M., and Llorens-Cortes, C. (2014) Biased signaling favoring gi over β-arrestin promoted by an apelin fragment lacking the C-terminal phenylalanine. *J. Biol. Chem.* **289**, 24599–24610
9. El Messari, S., Iturrioz, X., Fassot, C., De Mota, N., Roesch, D., and Llorens-Cortes, C. (2004) Functional dissociation of apelin receptor signaling and endocytosis: implications for the effects of apelin on arterial blood pressure. *J. Neurochem.* **90**, 1290–1301
10. Evans, N. A., Groarke, D. A., Warrack, J., Greenwood, C. J., Dodgson, K., Milligan, G., and Wilson, S. (2001) Visualizing differences in ligand-induced beta-arrestin-GFP interactions and trafficking between three recently characterized G protein-coupled receptors. *J. Neurochem.* **77**, 476–485
11. Reaux, A., De Mota, N., Skultetyova, I., Lenkei, Z., El Messari, S., Gallatz, K., Corvol, P., Palkovits, M., and Llorens-Cortès, C. (2001) Physiological role of a novel neuropeptide, apelin, and its receptor in the rat brain. *J. Neurochem.* **77**, 1085–1096
12. Reaux, A., Gallatz, K., Palkovits, M., and Llorens-Cortes, C. (2002) Distribution of apelin-synthesizing neurons in the adult rat brain. *Neuroscience* **113**, 653–662
13. O'Carroll, A. M., Selby, T. L., Palkovits, M., and Lolait, S. J. (2000) Distribution of mRNA encoding B78/apj, the rat homologue of the human APJ receptor, and its endogenous ligand apelin in brain and peripheral tissues. *Biochim. Biophys. Acta* **1492**, 72–80
14. Hus-Citharel, A., Bodineau, L., Frugière, A., Joubert, F., Bouby, N., and Llorens-Cortes, C. (2014) Apelin counteracts vasopressin-induced water reabsorption *via* cross talk between apelin and vasopressin receptor signaling pathways in the rat collecting duct. *Endocrinology* **155**, 4483–4493
15. Reaux-Le Goazigo, A., Morinville, A., Burlet, A., Llorens-Cortes, C., and Beaudet, A. (2004) Dehydration-induced cross-regulation of apelin and vasopressin immunoreactivity levels in magnocellular hypothalamic neurons. *Endocrinology* **145**, 4392–4400
16. Azizi, M., Iturrioz, X., Blanchard, A., Peyrard, S., De Mota, N., Chartrel, N., Vaudry, H., Corvol, P., and Llorens-Cortes, C. (2008) Reciprocal regulation of plasma apelin and vasopressin by osmotic stimuli. *J. Am. Soc. Nephrol.* **19**, 1015–1024
17. Blanchard, A., Steichen, O., De Mota, N., Curis, E., Gauci, C., Frank, M., Wuerzner, G., Kamenicky, P., Passeron, A., Azizi, M., and Llorens-Cortes, C. (2013) An abnormal apelin/vasopressin balance may contribute to water retention in patients with the syndrome of inappropriate antidiuretic hormone (SIADH) and heart failure. *J. Clin. Endocrinol. Metab.* **98**, 2084–2089
18. Lee, D. K., Cheng, R., Nguyen, T., Fan, T., Kariyawasam, A. P., Liu, Y., Osmond, D. H., George, S. R., and O'Dowd, B. F. (2000) Characterization of apelin, the ligand for the APJ receptor. *J. Neurochem.* **74**, 34–41
19. Tatemoto, K., Takayama, K., Zou, M. X., Kumaki, I., Zhang, W., Kumano, K., and Fujimiya, M. (2001) The novel peptide apelin lowers blood pressure *via* a nitric oxide-dependent mechanism. *Regul. Pept.* **99**, 87–92
20. Ishida, J., Hashimoto, T., Hashimoto, Y., Nishiwaki, S., Iguchi, T., Harada, S., Sugaya, T., Matsuzaki, H., Yamamoto, R., Shiota, N., Okunishi, H., Kihara, M., Umemura, S., Sugiyama, F., Yagami, K., Kasuya, Y., Mochizuki, N., and Fukamizu, A. (2004) Regulatory roles for APJ, a seven-transmembrane receptor related to angiotensin-type 1 receptor in blood pressure *in vivo*. *J. Biol. Chem.* **279**, 26274–26279
21. Japp, A. G., Cruden, N. L., Amer, D. A., Li, V. K., Goudie, E. B., Johnston, N. R., Sharma, S., Neilson, I., Webb, D. J., Megson, I. L., Flapan, A. D., and Newby, D. E. (2008) Vascular effects of apelin *in vivo* in man. *J. Am. Coll. Cardiol.* **52**, 908–913
22. Japp, A. G., Cruden, N. L., Barnes, G., van Gemeren, N., Mathews, J., Adamson, J., Johnston, N. R., Denvir, M. A., Megson, I. L., Flapan,

A. D., and Newby, D. E. (2010) Acute cardiovascular effects of apelin in humans: potential role in patients with chronic heart failure. *Circulation* **121**, 1818–1827
23. Ashley, E. A., Powers, J., Chen, M., Kundu, R., Finsterbach, T., Caffarelli, A., Deng, A., Eichhorn, J., Mahajan, R., Agrawal, R., Greve, J., Robbins, R., Patterson, A. J., Bernstein, D., and Quertermous, T. (2005) The endogenous peptide apelin potently improves cardiac contractility and reduces cardiac loading *in vivo*. *Cardiovasc. Res.* **65**, 73–82
24. Berry, M. F., Pirolli, T. J., Jayasankar, V., Burdick, J., Morine, K. J., Gardner, T. J., and Woo, Y. J. (2004) Apelin has in vivo inotropic effects on normal and failing hearts. *Circulation* **110**, II187–II193
25. Kuba, K., Zhang, L., Imai, Y., Arab, S., Chen, M., Maekawa, Y., Leschnik, M., Leibbrandt, A., Markovic, M., Schwaighofer, J., Beetz, N., Musialek, R., Neely, G. G., Komnenovic, V., Kolm, U., Metzler, B., Ricci, R., Hara, H., Meixner, A., Nghiem, M., Chen, X., Dawood, F., Wong, K. M., Sarao, R., Cukerman, E., Kimura, A., Hein, L., Thalhammer, J., Liu, P. P., and Penninger, J. M. (2007) Impaired heart contractility in Apelin gene-deficient mice associated with aging and pressure overload. *Circ. Res.* **101**, e32–e42
26. Wang, W., McKinnie, S. M., Patel, V. B., Haddad, G., Wang, Z., Zhabyeyev, P., Das, S. K., Basu, R., McLean, B., Kandalam, V., Penninger, J. M., Kassiri, Z., Vederas, J. C., Murray, A. G., and Oudit, G. Y. (2013) Loss of apelin exacerbates myocardial infarction adverse remodeling and ischemia-reperfusion injury: therapeutic potential of synthetic apelin analogues. *J. Am. Heart Assoc.* **2**, e000249
27. Barnes, G. D., Alam, S., Carter, G., Pedersen, C. M., Lee, K. M., Hubbard, T. J., Veitch, S., Jeong, H., White, A., Cruden, N. L., Huson, L., Japp, A. G., and Newby, D. E. (2013) Sustained cardiovascular actions of APJ agonism during renin-angiotensin system activation and in patients with heart failure. *Circ Heart Fail* **6**, 482–491
28. Brame, A. L., Maguire, J. J., Yang, P., Dyson, A., Torella, R., Cheriyan, J., Singer, M., Glen, R. C., Wilkinson, I. B., and Davenport, A. P. (2015) Design, characterization, and first-in-human study of the vascular actions of a novel biased apelin receptor agonist. *Hypertension* **65**, 834–840
29. Hamada, J., Kimura, J., Ishida, J., Kohda, T., Morishita, S., Ichihara, S., and Fukamizu, A. (2008) Evaluation of novel cyclic analogues of apelin. *Int. J. Mol. Med.* **22**, 547–552
30. Jia, Z. Q., Hou, L., Leger, A., Wu, I., Kudej, A. B., Stefano, J., Jiang, C., Pan, C. Q., and Akita, G. Y. (2012) Cardiovascular effects of a PEGylated apelin. *Peptides* **38**, 181–188
31. McKeown, S. C., Zecri, F. J., Fortier, E., Taggart, A., Sviridenko, L., Adams, C. M., McAllister, K. H., and Pin, S. S. (2014) The design and implementation of a generic lipopeptide scanning platform to enable the identification of 'locally acting' agonists for the apelin receptor. *Bioorg. Med. Chem. Lett.* **24**, 4871–4875
32. Fan, X., Zhou, N., Zhang, X., Mukhtar, M., Lu, Z., Fang, J., DuBois, G. C., and Pomerantz, R. J. (2003) Structural and functional study of the apelin-13 peptide, an endogenous ligand of the HIV-1 coreceptor, APJ. *Biochemistry* **42**, 10163–10168
33. Mitra, A., Katovich, M. J., Mecca, A., and Rowland, N. E. (2006) Effects of central and peripheral injections of apelin on fluid intake and cardiovascular parameters in rats. *Physiol. Behav.* **89**, 221–225
34. Murza, A., Belleville, K., Longpré, J. M., Sarret, P., and Marsault, É. (2014) Stability and degradation patterns of chemically modified analogs of apelin-13 in plasma and cerebrospinal fluid. *Biopolymers* **102**, 297–303
35. Murza, A., Besserer-Offroy, É., Côté, J., Bérubé, P., Longpré, J. M., Dumaine, R., Lesur, O., Auger-Messier, M., Leduc, R., Sarret, P., and Marsault, É. (2015) C-terminal modifications of apelin-13 significantly change ligand binding, receptor signaling, and hypotensive action. *J. Med. Chem.* **58**, 2431–2440
36. Fosgerau, K., and Hoffmann, T. (2015) Peptide therapeutics: current status and future directions. *Drug Discov. Today* **20**, 122–128
37. Vlieghe, P., Lisowski, V., Martinez, J., and Khrestchatisky, M. (2010) Synthetic therapeutic peptides: science and market. *Drug Discov. Today* **15**, 40–56
38. Llorens-Cortes, C., Bonnet, D., and Iturrioz, X. (2016), inventors, INSERM, assignee. Metabolically stable apelin analogs in the treatment of disease mediated by the apelin receptor. Patent WO2016102648 A1. June 30, 2016
39. Gerbier, R., Leroux, V., Couvineau, P., Alvear-Perez, R., Maigret, B., Llorens-Cortes, C., and Iturrioz, X. (2015) New structural insights into the apelin receptor: identification of key residues for apelin binding. *FASEB J.* **29**, 314–322
40. Dabiré, H., Barthélémy, I., Blanchard-Gutton, N., Sambin, L., Sampedrano, C. C., Gouni, V., Unterfinger, Y., Aguilar, P., Thibaud, J. L., Ghaleb, B., Bizé, A., Pouchelon, J. L., Blot, S., Berdeaux, A., Hittinger, L., Chetboul, V., and Su, J. B. (2012) Vascular endothelial dysfunction in Duchenne muscular dystrophy is restored by bradykinin through upregulation of eNOS and nNOS. *Basic Res. Cardiol.* **107**, 240
41. Reaux, A., Fournie-Zaluski, M. C., David, C., Zini, S., Roques, B. P., Corvol, P., and Llorens-Cortes, C. (1999) Aminopeptidase A inhibitors as potential central antihypertensive agents. *Proc. Natl. Acad. Sci. USA* **96**, 13415–13420
42. Krieg, E., Weissman, H., Shimoni, E., Bar On Ustinov, A., and Rybtchinski, B. (2014) Understanding the effect of fluorocarbons in aqueous supramolecular polymerization: ultrastrong noncovalent binding and cooperativity. *J. Am. Chem. Soc.* **136**, 9443–9452
43. Hus-Citharel, A., Bouby, N., Frugière, A., Bodineau, L., Gasc, J. M., and Llorens-Cortes, C. (2008) Effect of apelin on glomerular hemodynamic function in the rat kidney. *Kidney Int.* **74**, 486–494
44. Murza, A., Parent, A., Besserer-Offroy, E., Tremblay, H., Karadereye, F., Beaudet, N., Leduc, R., Sarret, P., and Marsault, É. (2012) Elucidation of the structure-activity relationships of apelin: influence of unnatural amino acids on binding, signaling, and plasma stability. *ChemMedChem* **7**, 318–325
45. Wang, W., McKinnie, S. M., Farhan, M., Paul, M., McDonald, T., McLean, B., Llorens-Cortes, C., Hazra, S., Murray, A. G., Vederas, J. C., and Oudit, G. Y. (2016) Angiotensin-converting enzyme 2 metabolizes and partially inactivates Pyr-Apelin-13 and Apelin-17: physiological effects in the cardiovascular system. *Hypertension* **68**, 365–377
46. Zhang, Y., Maitra, R., Harris, D. L., Dhungana, S., Snyder, R., and Runyon, S. P. (2014) Identifying structural determinants of potency for analogs of apelin-13: integration of C-terminal truncation with structure-activity. *Bioorg. Med. Chem.* **22**, 2992–2997
47. Katugampola, S. D., Maguire, J. J., Kuc, R. E., Wiley, K. E., and Davenport, A. P. (2002) Discovery of recently adopted orphan receptors for apelin, urotensin II, and ghrelin identified using novel radioligands and functional role in the human cardiovascular system. *Can. J. Physiol. Pharmacol.* **80**, 369–374
48. Japp, A. G., and Newby, D. E. (2008) The apelin-APJ system in heart failure: pathophysiologic relevance and therapeutic potential. *Biochem. Pharmacol.* **75**, 1882–1892
49. Folino, A., Montarolo, P. G., Samaja, M., and Rastaldo, R. (2015) Effects of apelin on the cardiovascular system. *Heart Fail. Rev.* **20**, 505–518

Received for publication July 8, 2016.
Accepted for publication October 24, 2016.

THE FASEB JOURNAL
The Journal of the Federation of American Societies for Experimental Biology

Development of original metabolically-stable apelin-17 analogs with diuretic and cardiovascular effects

Romain Gerbier, Rodrigo Alvear-Perez, Jean-Francois Margathe, et al.

FASEB J published online November 4, 2016
Access the most recent version at doi:10.1096/fj.201600784R